Fluorescence Intensity of Dye Containing Latex Particles Studied by Near-Field Scanning Optical Microscopy

Karin Jeuris, Peter Vanoppen, and Frans C. De Schryver*

Department of Chemistry, Katholieke Universiteit Leuven, Celestijnenlaan 200F, 3001 Heverlee-Leuven, Belgium

Johannes W. Hofstraat, Leo G. J. van der Ven, and Jan W. van Velde

Akzo Nobel Central Research, Department RGL, P.O. Box 9300, 6800 SB Arnhem, The Netherlands

Received May 29, 1998

ABSTRACT: Latex particles of various sizes, containing a fluorescent dye and dispersed at low density in a poly(vinyl alcohol) matrix, were imaged by near-field scanning optical microscopy. The fluorescence intensity of the latex particles was studied quantitatively, by integrating the total intensity measured per particle. For all the samples, a high accuracy in determination of the fluorescence intensity could be achieved. The noticed difference in fluorescence intensity for particles of a similar size is mainly affected by the size distribution of the particles and by sample preparation. Particularly, the smaller particles (50−100 nm) show a significant difference in fluorescence intensity. This was confirmed by further study of the distribution of particle sizes by transmission electron microscopy and by examination of the correlation between the fluorescence intensity of the latex particles and their size. When the size difference is significant (e.g., when particles of 100 and 200 nm, which show a narrow size distribution, are present in the same sample), the two types of particles can be clearly distinguished. Furthermore, for smaller particles (50 and 100 nm) the differences in depth position in the film lead to differences in emission intensity.

Introduction

Polymer particles are an important class of materials, which find application in a wide range of areas. In coatings they are applied in water-based formulations[1,2] and in powder coatings.[3] In pharmaceutical applications polymer particles are used in diagnostics[4,5] and in cell separation.[6] Polymer particles are also applied in adhesives and sealants and in rheology modifiers.[7] Recently, polymer particles have found use in combinatorial chemistry.[8]

In most applications the polymer particles have sizes that are below 1 μm, so their characterization is far from straightforward. Morphological properties can be evaluated by means of electron microscopy. However, no good techniques are available for the characterization of their chemical structure. It is the chemical nature of the particles that determines to a great extent their properties. Functional groups largely determine the chemical properties of materials; it is the identity, spatial distribution, and concentration of functional groups that determine the chemical structure of polymer particles and important functions as adhesion, possibilities for further reaction (coupling, cross-linking reactions, interfacial effects). For most applications mentioned above, polymer particles with tailor-made functionality have been developed.

The goal of the present study is to investigate whether near-field scanning optical microscopy can be applied to determine optical images of submicrometer polymer particles. The study of fluorescent labeled polymer particles is interesting as such, since one may observe interactions of the particles and their environment, or between particles, directly. Also, functional groups may be labeled with suitable, specifically reactive fluorescent probes, so that it may become possible to determine the location and concentration of functional groups on polymer latices in this way.

Near-field scanning optical microscopy (NSOM) is an optical scanning probe microscopy technique that, by illumination of the sample through an aperture of subwavelength size, breaks the diffraction limit ($\lambda/2$), limiting the resolution of conventional optical microscopy. The most widely used subwavelength light source consists of a tapered optical fiber that is subsequently coated with aluminum, creating a small aperture at the end point of the fiber. The lateral position of the sample is raster scanned while maintaining a fixed distance of a few nanometers between the sample and NSOM probe via regulation of the force between the fiber and the sample.[9] This shear-force method allows simultaneous determination of the topographical structure and of the optical properties of the sample. More detailed information on the basic aspects of this method and its instrumentation have been reported previously.[10−12]

The detection and spectroscopic analysis of the fluorescence of structures down to single molecules have been studied in detail using NSOM.[13−16] Fluorescence mapping of heterogeneous organic films, like Langmuir−Blodgett films[17] or films consisting of J-aggregates,[18,19] micrometer-sized porphyrin wheels,[20] conjugated polymers,[21,22] or latex particles,[12] are reported in the literature.

In the present contribution, we report a study by NSOM of the parameters influencing the fluorescence intensity of latex particles, containing fluorescent dyes.

Experimental Section

The polymer films studied were prepared from dilute solutions of latex particles and poly(vinyl alcohol) (PVA) in such a way that thin films are obtained which contain isolated

* To whom correspondence should be addressed.

10.1021/ma980855k CCC: $15.00
Published on Web 11/07/1998

Table 1. Overview of the Size of the Studied Particles with Average Diameters and Standard Deviations, As Specified by the Supplier and Measured with a TEM Apparatus

	molecular probes			polysciences	
size, nm	av diameter, nm	std dev, nm	no. of fluorophores/ particle	av diameter, nm	std dev, nm
Specifications Given by the Suppliers					
50				64	10 (16%)
100	110	22 (20%)	7.4×10^3	84	8 (10%)
200	220	44 (20%)	1.1×10^5	213	8 (4%)
Results of TEM Analysis					
50				46	13 (30%)
100	99	5 (5%)		83	11 (13%)
200	224	10 (4.5%)		213	8 (4%)

particles. The films, which have a thickness of approximately 30−40 nm, are prepared by spin-coating. The first set of polystyrene particles was acquired from Molecular Probes. They contain a yellow-green fluorescent dye, which can be excited very efficiently at 488 nm, while the maximum of emission is situated at 515 nm. Particles with two different sizes, 100 and 200 nm, have been used. A variation of the size of the particles of ±5% was specified by the supplier. Another set of polystyrene latex particles was obtained from Polysciences. These particles are labeled with a green fluorescent dye, with an excitation maximum situated at 460 nm and an emission maximum at 480 nm. In this case, three different particle sizes, 50, 100, and 200 nm, were used. Polysciences specifies a margin on these size values of a few percent. In Table 1, an overview is given of all the particles investigated in this study.

The NSOM instrument is a modified Topometrix Aurora. The 670 nm diode laser for shear-force feedback was replaced with a 980 nm diode laser in order to allow the detection of fluorescence up to wavelengths around 800 nm. Additionally, the PMT detector of the Aurora was replaced by a more sensitive detector with lower background, i.e., a single-photon-counting avalanche photodiode module (EG&G, model SPCM-200-CD1718).

The 458 nm line from an argon ion laser was used as excitation source. The laser light was coupled into the NSOM fiber probe via a single-mode fiber coupler. The output intensity (measured in the far field) from the probe was typically several nanowatts. The excitation light was excluded from reaching the detector by a holographic laser notch filter (Kaiser Optical Systems). Additional IR short pass filters (CVI SPF-900) were employed to block the shear-force laser light. The fluorescence light was collected in transmission mode with a dry objective (Zeiss ×63, NA 0.85). The total experimental setup is discussed in detail elsewhere.[23] The scan speed was typically 2 μm/s for a 10 × 10 μm scan range, while the resolution was never less than 200 × 200 pixels.

The tip is the crucial part of a NSOM, because its dimensions determine to a great extent the spatial resolution of the microscope. Furthermore, the shape of the tip is also of great importance, because it determines the throughput of excitation light. To control better the size and shape of the tips, homemade NSOM probes were employed in the experiments. They were made using the heating and pulling method. The resulting tapered fibers are coated with a layer of aluminum, leaving the end face uncoated.[24,25] The aperture size varies between 50 and 120 nm in diameter.

TEM measurements were done with a Philips EM 400. The suspension with particles was diluted and sprayed on a carbon grid after dilution to such an extent that isolated particles were obtained. The images were analyzed with a Context Vision image analysis instrument; typically 100−200 particles were analyzed. The accuracy of the particle size measurement is better than 5%.

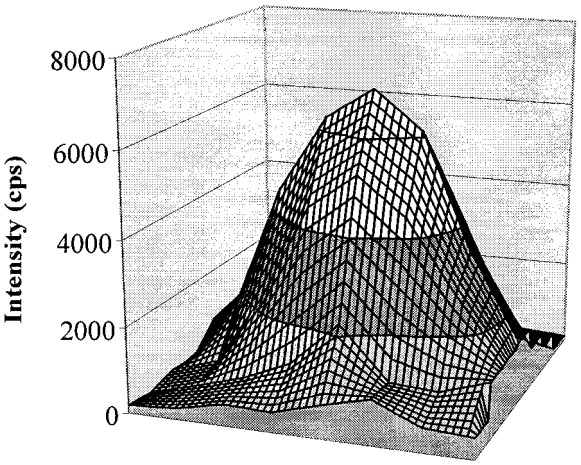

Figure 1. Three-dimensional plot of the intensity distribution of one bead, cut out of the NSOM image. The axes in the *x* and *y* plane correspond to a certain amount of pixels, depending on the particle size, which are chosen in such a way that the size of the excision is constant within one image. To calculate the integrated intensity, the volume under this surface is integrated.

Results and Discussion

A detailed analysis of the fluorescence intensity of dye-labeled latex particles was performed. In such a study, one can only compare the fluorescence intensities of different particles in one image. The absolute intensities of different images cannot be compared, not only because the intensity of the excitation light exciting the sample is never exactly the same, certainly not when different tips are used, but also because the detection efficiency is different for each experiment. Therefore, films with mixtures of particles with different sizes were prepared, which allows the comparison of the relative fluorescence intensity of the individual particles, because the same tip is used to image all the particles.

Samples containing latex particles with sizes of 100 and 200 nm, received from Molecular Probes, were imaged. First, samples with particles of one size and, in a later stage, samples with a mixture of different particle sizes were examined. To calculate the integrated intensity, the fluorescence signal of each particle is cut out of the fluorescence image, and a three-dimensional plot is made from this excision. An example of such a plot is shown in Figure 1. The volume under this plot is integrated, which allows the calculation of the integrated intensity per particle, in counts per second. These calculated integrated intensities are corrected for the background signal, by cutting out an equal area of the background. The size of all the excisions in one image is the same and is chosen in such a way that the fluorescence signal of the largest particle fits in. This excision method assumes that the intensity is in the linear response threshold of the image. The dynamic range (0−100 000 counts per second) was checked using a set of neutral density filters and was found to be linear.

First, a series of measurements was performed to discriminate between sample and instrumental effects. For all samples measured, a difference in integrated intensity was noted for particles of a similar size. The reproducibility of the measurement and of the data processing was examined.

In Figure 2, a topographic and a fluorescence image are given of a sample containing 100 nm particles. The

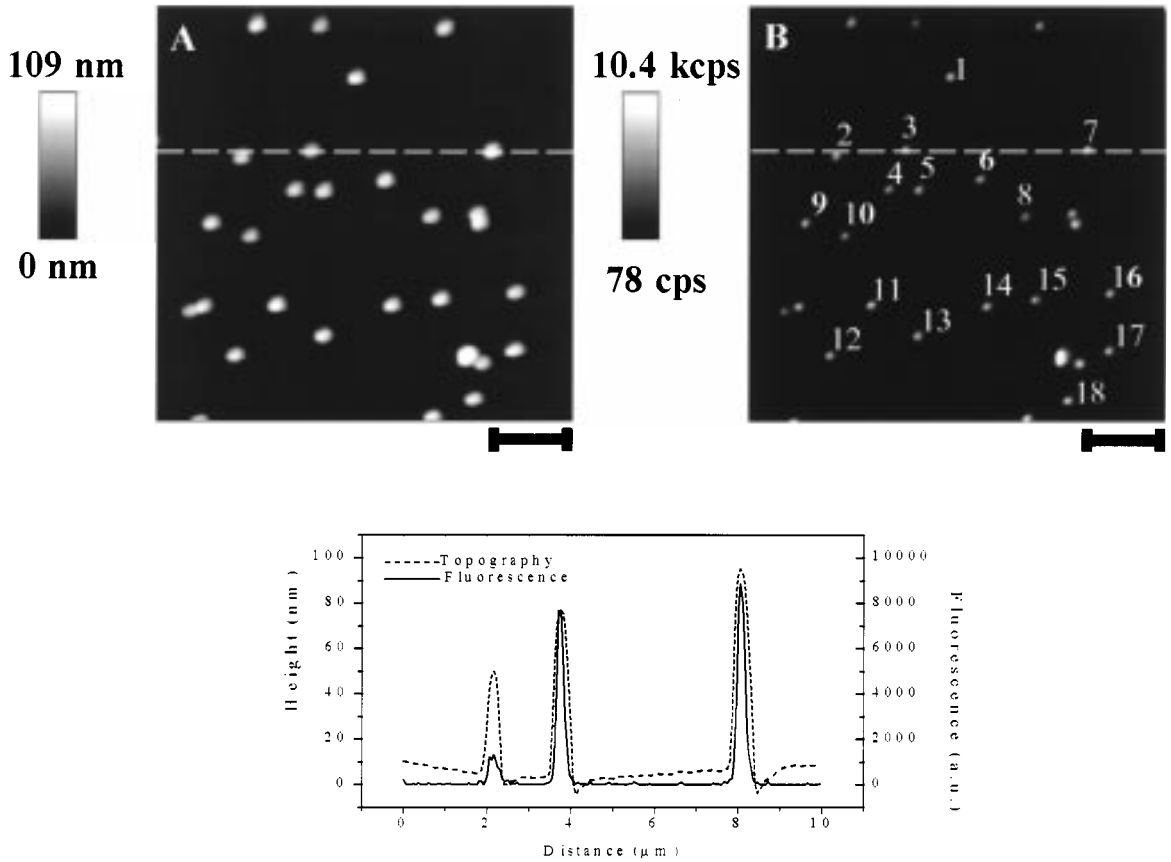

Figure 2. Topographic (A) and fluorescence (B) images of 100 nm latex particles in a PVA matrix. The scale bar below each image represents 2 μm. Individual particles used to discriminate between instrumental and sample effects are indicated with a number. Line scans are shown, taken through the topography and fluorescence image; they are marked with a white dashed line.

line scan through this image shows that the topographic and fluorescence signals overlap well, but the width of the fluorescence signal is narrower than the topography profile. The width of the particles in the topography image is about 400 nm, in the fluorescence image the width is about 250 nm. The width in the topography image is larger as a result of the amount of aluminum deposited on the tip end. In both images the width is broader than the real particle size because of tip convolution.

To check the reproducibility of the measurement, a well-defined area of the sample (10 by 10 μm) was scanned five consecutive times with the same tip, without optimizing the excitation light between the different scans. For these five images, the integrated intensity was calculated for 18 different particles in the image. The fluorescence image of the area used for these calculations is shown in Figure 2B; the individual particles are marked with a number. A plot with the absolute and normalized intensities is given in Figure 3. The intensity plot in Figure 3A clearly shows that there is a trend in the fluorescence intensity measured for the different particles. When going from scan one to five, the fluorescence intensity first shows an increase, and subsequently the intensity decreases for most of the particles. This decrease in intensity is not due to bleaching. A bleaching experiment showed that bleaching only occurs when the same spot is continuously illuminated for at least 30−40 min. This is not the case during scanning, since a 100 nm bead is only illuminated for about 0.6 s per scan. This suggests that relaxation of the fiber couplers leads to a decrease in excitation energy. In the NSOM setup, three fiber couplers are used to couple the excitation light into the NSOM probe.

The intensity data (Figure 3B), normalized with respect to the intensity values of one particle, show that the intensity does not change substantially over the five measurements, when taking into account the relaxation of the couplers. For the five measurements of one particle the standard deviation is about 0.5×10^6 cps (8%) for an average intensity of 6.3×10^6 cps. For one measurement of the eighteen particles the standard deviation is about 0.8×10^6 cps (13%). So it is clear that the fluctuation in intensity for one particle over the five measurements is smaller than the fluctuation in intensity between the particles in one measurement. The differences in intensity between the particles in one image are therefore too large to be caused by an instrumental effect. Thus, it can be concluded that the differences in intensity, measured in one image, are inherent to the investigated sample.

The second point that was evaluated, is the reproducibility of data processing. In one image, the procedure of cutting out one particle and calculating the integrated intensity, was repeated six times to check if the process of data handling itself creates differences in intensity. The calculations showed that the integrated intensities were the same, within a small margin (±1%).

For all samples containing only particles of one size, 100 or 200 nm, a difference in intensity was noted. A topographic and fluorescence image of a 100 nm sample is given in Figure 2, a fluorescence image of the samples containing 200 nm particles is shown in Figure 4. The integrated intensities obtained from integration of the

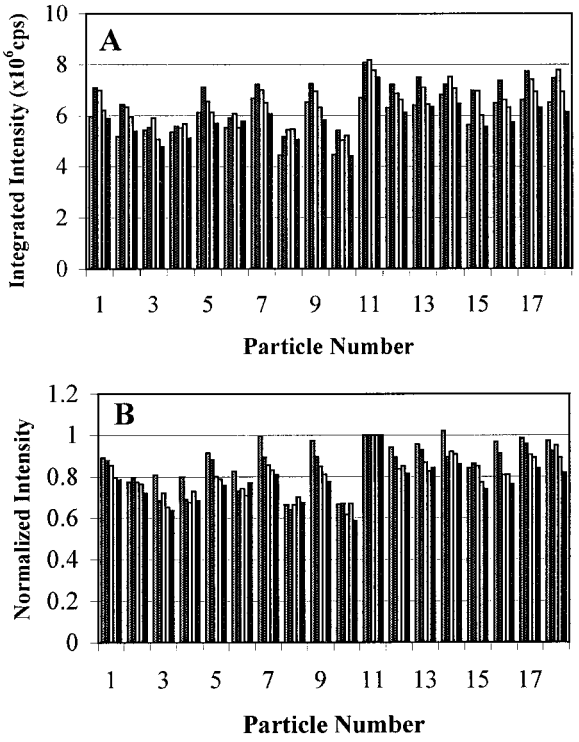

Figure 3. Discrimination between instrumental and sample effects: (A) integrated intensities for five consecutive measurements, calculated for 18 different particles; (B) intensities for these five measurements, normalized with respect to the values of particle number 11.

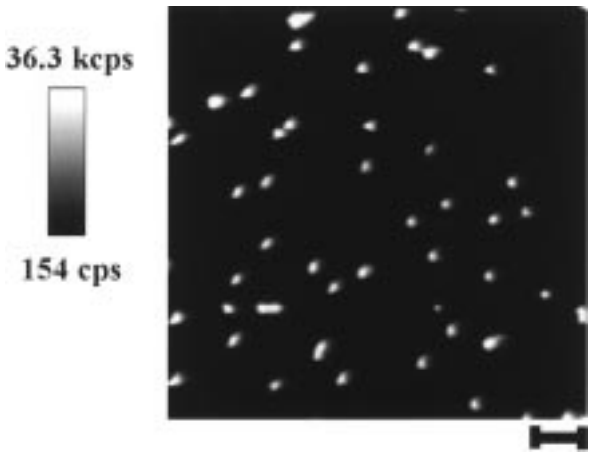

Figure 4. Fluorescence image of a sample containing 200 nm latex particles. The scale bar below the image represents 2 μm.

data of a number of individual particles are given in Figure 5. For the 100 nm particles the average value is 6.7×10^6 cps, with a standard deviation of 12%. For the 200 nm particles the average value is 19.2×10^6 cps, with a standard deviation of 13%. All numbers and results are listed in Table 2. In a first approximation, it may be assumed that the amount of fluorophore per particle varies linearly with the volume. To determine the volume of the actual particles used in the quantitative fluorescence measurements, a TEM analysis has been performed. The results show a variation of 5 nm on the 100 nm particles with an average diameter of 99 nm, and a variation of 10 nm on the 200 nm beads with an average diameter of 224 nm. The variations in size therefore seem to be smaller than the values specified by Molecular Probes. The volume of the

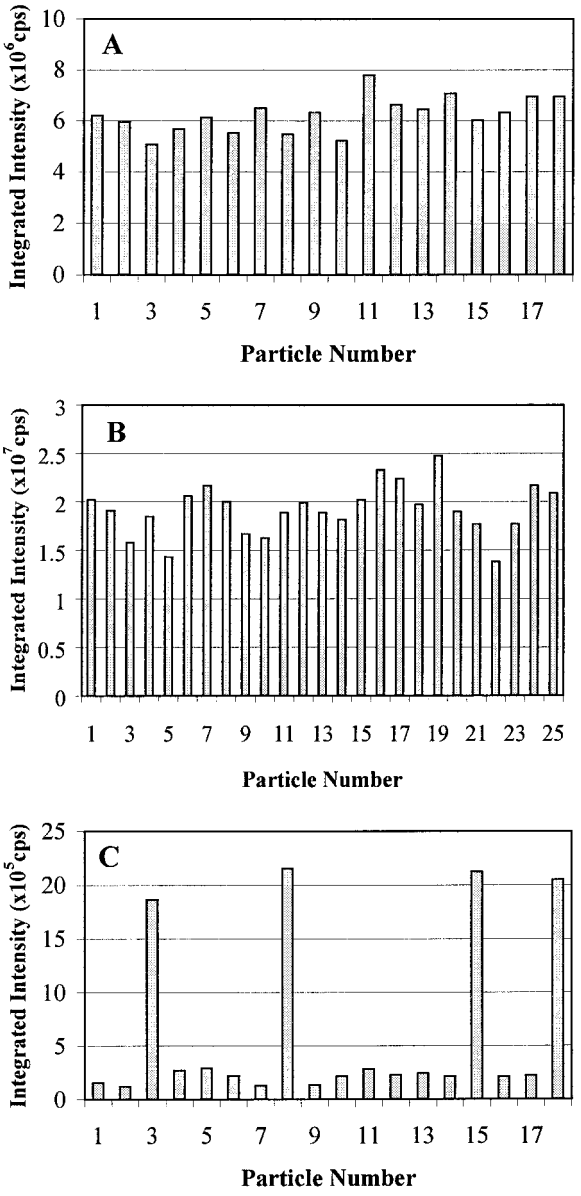

Figure 5. Integrated intensities as a function of the particle number. (A) Integrated intensities for the 100 nm particles, (B) integrated intensities for the 200 nm particles, and (C) integrated intensities for the sample containing a mixture of two different particle sizes, 100 and 200 nm.

Table 2. Overview of Data of the Particles from Molecular Probes

	100 nm	200 nm
fluorescence intensity (cps)	$6.7 \times 10^6 \pm 0.8 \times 10^6$ (12%)	$19.2 \times 10^6 \pm 2.6 \times 10^6$ (13%)
av diameter (nm)	99 ± 5 (5%)	224 ± 10 (4.5%)
calcd vol (nm^3)	$5.1 \times 10^5 \pm 0.8 \times 10^5$ (16%)	$5.85 \times 10^6 \pm 0.85 \times 10^6$ (15%)

particles was calculated using the results of the TEM measurements. For the 100 nm particles a volume of 5.1×10^5 nm^3 was found with a standard deviation of 16%. For the 200 nm particles a volume of 5.85×10^6 nm^3 was calculated, with a standard deviation of 15%. For both the 100 and 200 nm particles the distribution in volume and intensity does correspond. The results show that the variations in intensity to a large extent can be explained by the variations in size.

The correlation between height and integrated intensity was investigated for the films containing 100 or 200

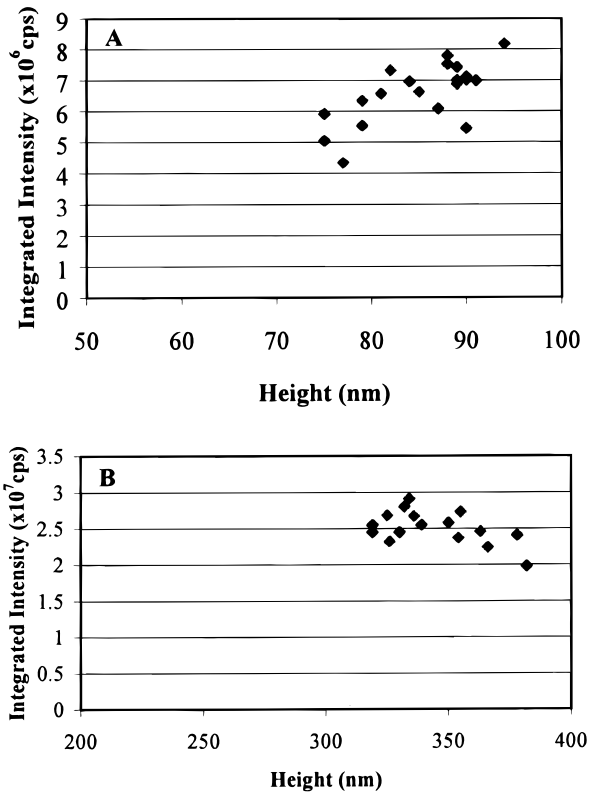

Figure 6. Correlation between the integrated intensities and the height of the particles. The plots are shown for the 100 nm (A) and the 200 nm (B) particles.

nm latex particles. The fluorescence image of the area where this parameter was examined for the 100 nm particles is shown in Figure 2B. There is a correlation between the height and the integrated intensity, as is shown in Figure 6A. For the 200 nm particles, the results show that the effect of the PVA film thickness is much less pronounced (Figure 6B). Two effects can give an explanation for this correlation, i.e., the direct effect of the difference in particle diameter and, second, an additional effect of incorporation of the particle in the PVA matrix. This effect of incorporation in the PVA matrix is more likely for the smaller particles than for the larger particles because of the PVA film thickness. Generally, one may expect that the particles that are deeper embedded in the PVA matrix show less fluorescence and that the particles sticking out show more fluorescence.

A fluorescence image of the sample containing a mixture of particles is given in Figure 7, the integrated intensities are shown in Figure 5C. For this sample, a distinct difference in intensity for the 100 and 200 nm particle sizes is noticed. For both sizes, some statistical parameters were obtained. The average intensity value for the 100 nm particles is 0.21×10^6 cps, with a standard deviation of 28%; for the 200 nm particles the average value is 2.15×10^6 cps, with a standard deviation of 5%. The difference in intensity between both particle sizes is approximately a factor 10. This factor is slightly smaller than the ratio of the volumes, calculated from the average diameters as found in the TEM measurements, i.e., a factor of 12. This deviation to a lower value can be due to the fact that the total volume of the 200 nm particles is not excited completely. The intensity of the near-field is decreasing very rapidly with the distance and is negligible at a distance of 200 nm. The results show that the amount of chromophores

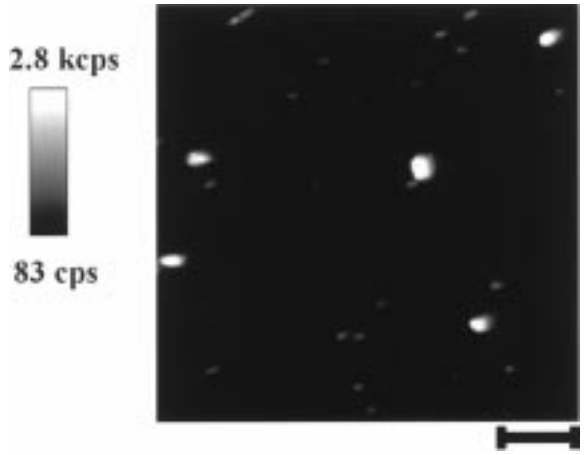

Figure 7. Fluorescence image of a sample containing a mixture of 100 and 200 nm particles. The scale bar below the image represents 2 μm.

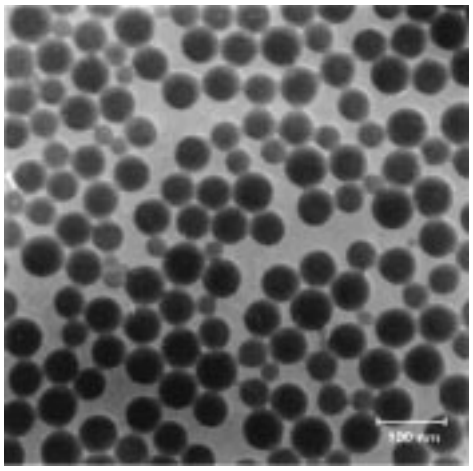

Figure 8. TEM image of latex particles for which the supplier specifies an average diameter of 64 nm with a standard deviation of 10 nm. However, the TEM measurements result in an average diameter of 46 nm with a standard deviation of 13 nm.

is proportional to the volume of the particles. This points out that the distribution of the chromophores in the particles is quite homogeneous. This is further confirmed by the fact that if the chromophores were only situated at the surface of the particles, the ratio of the intensities would be equal to a factor 5. The possible incomplete excitation of the 200 nm particles has a negligible influence on the statistical distribution, as is proven by the fact that the distribution of the intensities is of the same order of magnitude for the 100 and the 200 nm particles, as is mentioned before.

For the batch of polystyrene particles from Polysciences, comparable experiments were performed. For the samples containing particles of 50 or 100 nm, a rather large fluctuation in integrated intensity is noticed. These intensity differences are to a large extent due to the more heterogeneous distribution in size. TEM measurements indicated that, in particular for the smaller particles, the size variations were more pronounced than specified. For the 50 nm particles, a size of 46 ± 13 nm was found (Figure 8) and for the 100 nm particles a size of 83 ± 11 nm. On the basis of these TEM measurements, it is clear that for a mixture of 50 and 100 nm particles there is an almost continuous distribution in size between 35 and 95 nm. This continuous distribution in size is reflected in the con-

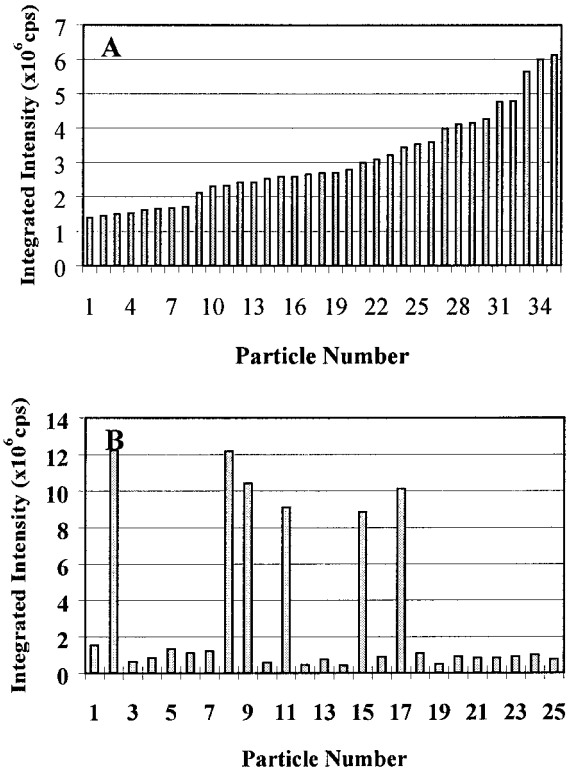

Figure 9. Integrated intensities as a function of the particle number for the second batch of latex particles (Polysciences): (A) integrated intensities for the sample containing a mixture of 50 and 100 nm particles; (B) integrated intensities for the sample containing a mixture of 100 and 200 nm particles.

tinuous distribution in fluorescence intensity, as shown in Figure 9A. However, for the samples containing 200 nm particles, the variation in intensity was less pronounced, which is in agreement with the results from the TEM measurements. Here, a size of 213 ± 8 nm was found for the 200 nm particles. For the mixture of 100 and 200 nm particles, in contrast to the mixture of 50 and 100 nm particles, a distinct difference in intensity is noted. The difference in intensity is approximately a factor 12. The plot of the integrated intensities for this mixture is given in Figure 9B.

Conclusions

A study on the correlation between the fluorescence intensity of dye-labeled latex particles and their size was performed using NSOM. For all samples, it was shown that a relatively high accuracy in determination of fluorescence intensity could be achieved. The variation in fluorescence intensity is mainly affected by the size distribution and by effects of sample preparation. Particularly the smaller particles (50−100 nm) show a significant difference in fluorescence intensity. This was confirmed by further study of the distribution of particle sizes by transmission electron microscopy and by examination of the correlation between the fluorescence intensity of the latex particles and their size. When the height of the particles is much larger than the thickness of the film, the PVA matrix does not influence the intensity, but for smaller particles, the differences in depth position in the film lead to differences in emission intensity. The results clearly show that it is possible to distinguish and analyze particles of different sizes in a mixture.

Acknowledgment. This work was supported by FWO and DWTC through IUAP-4-11. P. van Blokland and C. van der Meij-Bruin are gratefully acknowledged for the TEM measurements.

References and Notes

(1) Verkholantsev, V. V. *Eur. Coat. J.* **1997**, 1036.
(2) Waters, J. A. In *Polymeric Dispersions: Principles and Applications*; NATO ASI Series, Series E, Vol. 335; Plenum: New York, p 421.
(3) Verkholantsev, V. V. *Eur. Coat. J.* **1998**, 360.
(4) Ugelstad, J.; Stenstad, P.; Kilaas, L.; Prestvik, W. S.; Rian, A.; Nustad, K.; Herge, R.; Berge, A. *Macromol. Symp.* **1996**, *101*, 491.
(5) Javier Gella, F.; Serra, J.; Gener, J. *Pure Appl. Chem.* **1991**, 63, 1131.
(6) Prestvik, W. S.; Berge, A.; Mork, P. C.; Stenstad, P. M.; Ugelstad, *J. Proceedings of the 1st International Conference on Scientific Clinical Application of Magnetic Carriers*; Haefeli, U., Ed.; Plenum Press: New York, 1997; p 11.
(7) Defusco, A. J.; Seghal, K. C.; Bassett, D. R. In *Polymeric Dispersed Applications*; NATO ASI Series, Series E, Vol. 335; Plenum: New York, p 379.
(8) Smith, M. *Recherche* **1997**, 48.
(9) Betzig, E.; Finn, P. L.; Weiner, J. S. *Appl. Phys. Lett.* **1992**, *60*, 2482.
(10) For an introduction see, e.g.; (a) Courjon, D.; Bainier, C. *Rep. Prog. Phys.* **1994**, 57, 989. (b) Pohl, D. W.; Courjon, D. In *Near-field Optics*; NATO ASI Series, Series E 242; Kluwer: Dordrecht, The Netherlands, 1993. (c) Paesler, M. A.; Moyer, P. J. In *Near-field Optics, theory, instrumentation, and applications*; John Wiley & Sons, Inc.: New York, 1997.
(11) Betzig, E.; Trautman, J. K. *Science* **1992**, *257*, 189.
(12) Rücker, M.; Vanoppen, P.; De Schryver, F. C.; Ter Horst, J. J.; Hotta, J.; Masuhara, H. *Macromolecules* **1995**, *28*, 7530.
(13) Betzig, E.; Chichester, R. J. *Science* **1993**, *262*, 1422.
(14) Trautman, J. K.; Macklin, J. J.; Brus, L. E.; Betzig, E. *Nature* **1994**, *369*, 40.
(15) Xie, S. X.; Dunn, R. C. *Science* **1994**, *265*, 361.
(16) Ambrose, W. P.; Goodwin, P. M.; Martin, J. C.; Keller R. A. *Science* **1994**, *265*, 364.
(17) Brunner, R.; Bietsch, A.; Hollricher, O.; Marti, O.; Lambacher, A. *Surf Int. Anal.* **1997**, *25*, 492.
(18) Vanden Bout, D. A.; Kerimo, J.; Higgins, D. A.; Barbara, P. F. *Acc. Chem. Res.* **1997**, *30*, 204.
(19) Higgins, D. A.; Kerimo, J.; Vanden Bout, D. A.; Barbara, P. F. *J. Am. Chem. Soc.* **1996**, *118*, 4049.
(20) Hofkens, J.; Latterini, L.; Vanoppen, P.; Faes, H., Jeuris, K.; De Feyter, S.; Kerimo, J.; Barbara, P. F.; De Schryver, F. C.; Rowan, A. E.; Nolte, R. M. J. *J. Phys. Chem. B* **1997**, *101*, 10589.
(21) Wei, P.-K.; Hsu, J.-H.; Fann, W.; Chuang, K.-R.; Lee, H.-T.; Chen, S.-A. *Appl. Opt.* **1997**, *36*, 3301.
(22) DeAro, J. A.; Weston, K. D.; Buratto, S. K.; Lemmer, U. *Chem. Phys. Lett.* **1997**, *277*, 532.
(23) Vanoppen, P.; Hofkens, J.; Latterini, L.; Jeuris, K.; Faes, H.; Kerimo, J.; Barbara, P. F.; Rowan, A. E.; Nolte, R. J. M.; De Schryver, F. C. In *Applied fluorescence in chemistry, biology, and medicine*; Rettig, W., Strehmel, B., Schrader, S., Eds.; Springer-Verlag (in press).
(24) Valaskovic, G. A.; Holton, M.; Morrison, G. H. *Appl. Opt.* **1995**, *34*, 1215.
(25) Garcia-Parajo, M.; Tate, T.; Chen, Y. *Ultramicroscopy* **1995**, *61*, 155.

MA980855K